

Temperature Curling in Rigid Pavements: An Application of Dimensional Analysis

ANASTASIOS M. IOANNIDES AND RICARDO A. SALSILLI-MURUA

This paper presents a closed-form solution to the problem of a slab-on-grade under combined temperature and wheel loading, derived on the basis of finite element results. This solution is in the form of a multiplication factor (function of the temperature differential) to be applied to the Westergaard equation to determine the maximum combined tensile stress in the slab under edge loading. In addition, a sound, engineering approach to numerical, experimental, and field data interpretation is proposed, founded on the principles of dimensional analysis. In view of the wide variety of available data, including those from the Strategic Highway Research Program and from finite element studies, the major problem confronting the profession today is no longer one of data availability, but one of data interpretation. In addressing this problem, the general trend in the last three decades has been to show an overwhelming preference for, and an unlimited confidence in, the results of sophisticated statistical analyses, without much consideration of the underlying engineering interactions among the host of input parameters involved. Although in a highly empirical field such as the study of pavement behavior regression techniques will always be an invaluable tool, the profession can benefit immensely by using dimensional analysis to determine the engineering dependent and independent variables to be examined. Without such exercise of engineering judgment, regression is lamentably bound to remain just that.

An analytical solution to the problem of a rigid pavement slab-on-grade under the combined action of a temperature gradient and externally applied wheel loads has not been forthcoming in recent years, despite considerable progress achieved in related areas. The major reason for this shortfall is the complexity introduced by the loss of support experienced by a curled slab, thereby rendering the principle of superposition inapplicable. Thus, it has long been recognized that merely summing up the stresses due to the applied wheel loads and those induced by curling (1,2) is an inadequate and often erroneous approach (3,4).

An obvious recourse to the lack of a closed-form solution would be to use data obtained from finite element (FE) or other numerical procedures and to verify such predictions by comparing them to actual field observations. Sophisticated FE codes are currently available for routine execution and can provide an enormous amount of pertinent information in a reasonable amount of time. In parallel, the Strategic Highway Research Program (SHRP) promises to supply a large variety of carefully collected in situ data that could also be used in this respect. Thus, the problem confronting the profession today is no longer one of data availability, but one of

data interpretation. This paper addresses the issue of data interpretation using the principles of dimensional analysis for the case of the problem at hand, although the concepts presented are applicable to many other areas of scientific endeavor.

DIMENSIONAL ANALYSIS AND DATA INTERPRETATION

The need for dimensional analysis in those areas where available analytical tools are not capable of yielding exact solutions and which, therefore, are heavily involved with numerical and empirical work, is well recognized in several branches of engineering—most notably in fluid mechanics. Consider, for instance, the comments of Roberson and Crowe (5). They stress that in such fields, "it is essential that researchers employ dimensionless parameters [for] analyzing model studies and for correlating the results of experimental research." For example, "by considering a nondimensional form of Bernoulli's equation we will have made a tremendous reduction in experimental work from that required before considering the nondimensional form. The process of nondimensionalizing the equation reduces the correlating parameters from five to two."

As a result, considerable time savings are realized with respect to data collection, because the nondimensional factorial is much smaller than its dimensional counterpart. Note that as with the Bernoulli equation, it is often possible to have "a clue about the governing equation" from previous theoretical investigations, which may themselves be incomplete. Nonetheless, "by considering the dimensionless form of that equation, we [are] able to obtain a set of dimensionless parameters with which to correlate our data" (5).

Dimensional analysis is not unknown in transportation facilities studies. It is encountered in the works of such notable pioneers as Westergaard, Bradbury, Burmister, Odemark, Pickett, and Losberg, to name a few, although this is often done in passing and in a nonsystematic fashion. Burmister's work is a case in point.

In his classic paper (6), Burmister presented his two-layer system solution in terms of two dimensionless independent variables (E_1/E_2 and h/a) and one nondimensional dependent variable (F_w)—the latter being a correction factor for the existing one-layer, Boussinesq solution. Here, E_1 and E_2 are the moduli of the top and bottom layers, respectively, h is the thickness of the top layer, and a is the radius of the applied load.

Significantly less attention was drawn to Burmister's comments at the First International Conference on the Structural Design of Asphalt Pavements in 1962 (7). At that conference, he advocated that the "principles of dimensional analysis should be rigorously followed, involving fundamental dimensionless ratios which have physical significance." This approach not only provides a useful way to present theoretical and analytical data, but it is also "a more basic approach in a comprehensive evaluation of field data, leading to dimensionally correct empirical relations" (7).

The first step in applying the principles of dimensional analysis to pavement systems is to distinguish between input parameters and independent variables entering the analysis, as well as distinguishing between output values and dependent variables. It is often assumed that these pairs of terms have identical meanings, thus resulting in extremely long factorials and incomplete (often miscasting) data interpretation. Rauhut et al. (8), for example, conclude (in good humor) that "measuring all of the possible main effects and interactions between the 30 factors [involved in a typical execution of computer program VESYS] at two levels each would have required 2^{30} (slightly more than 10^9) separate observations." Regression algorithms obtained in this way cannot be applied to data other than the data for which the algorithms were developed.

In contrast, establishing independent and dependent variables, by combining a number of input parameters and output values into nondimensional forms, merely recognizes the fundamental engineering interactions between the factors involved. This is preferable to delegating this cardinal engineering task to the statistician or, more commonly, to the "black box" of sophisticated and complex statistical computer packages.

Previous investigations (9,10,11), showed how the Westergaard problem of a slab-on-grade can be reduced to a nondimensional equation of the form:

$$R^* = f(\log [a/l]) \quad (1)$$

where

- R^* = dimensionless response,
- f = logarithmic function of a/l sought,
- a = radius of the applied load, and
- l = radius of relative stiffness of slab-subgrade system, given by

$$l = [Eh^3\{12(1 - \mu^2)k\}]^{1/4} \quad (2)$$

where

- E = slab Young's modulus,
- h = slab thickness,
- μ = slab Poisson ratio, and
- k = modulus of subgrade reaction.

The well-known Westergaard equations essentially present the functional forms of f for the particular cases of the three primary maximum responses; namely, deflection, δ , bending stress, σ , and subgrade stress, q , for each of the three fundamental loading conditions (i.e., interior, edge, and corner). The nondimensional responses, R^* , can be extracted from these equations, as follows (12):

$$R^* = [\delta D/Pl^2] \text{ or } R^* = [\delta kl^2/P] \text{ for deflection,}$$

$$R^* = [q/l^2/P] \text{ for subgrade stress, and}$$

$$R^* = [\sigma h^2/P] \text{ for bending stress.} \quad (3)$$

In these responses, D is the flexural stiffness of the slab, which is equal to $Eh^3\{12(1 - \mu^2)\}$, and P is the total applied load.

Thus, five of Westergaard's six input parameters $\{E, \mu, h, k, \text{ and } a\}$ are lumped into a single nondimensional ratio, a/l , which defines uniquely each of the nondimensional responses, independent of the values of the individual parameters. Therefore, even though each particular input parameter may change, the nondimensional response of the system (which involves the sixth input parameter, P) is unaltered, if a/l remains constant. As in Bernoulli's problem, Westergaard's is thus reduced to one of a single independent variable, a/l , and three dependent variables (the three nondimensional responses).

Several extensions based on Westergaard's work are now possible. To account for the finite extent of concrete pavement slabs, Ioannides et al. (13) introduced the normalized length term, L/l , assuming that the width, W , of the slab was equal to its length, L . Thus, Westergaard's solutions may be corrected for the effect of slab size, using data from FE studies. Similarly, the effect of dual-wheel loads, may be quantified by S/a or S/l , where S is the spacing of the two loads (14).

Note that all independent variables, as well as all calculated responses are expressed in the form of nondimensional ratios. This allows results obtained from one given set of input parameters to be used to predict the response under a number of other combinations of parameters, giving the same independent variables. As a corollary, only a limited amount of data (obtained from FE studies, laboratory tests, or field observations) is sufficient to describe most pavements of practical interest.

IDENTIFYING THE INDEPENDENT VARIABLES FOR CURLING ANALYSIS

When considering the effects of a temperature gradient through the thickness of the slab, it is necessary to seek the nondimensional independent variables involved, in addition to a/l and L/l . Input parameters to this problem usually include the following:

- α = coefficient of thermal expansion of concrete, $LL^{-1} \cdot T^{-1}$,
- g = temperature gradient, TL^{-1} ,
- ΔT = temperature differential between top and bottom, T , and
- γ = unit weight of concrete, FL^{-3} .

Here the three primary or basic dimensions are abbreviated as length, L , force, F , and temperature, T .

Examining available analytical solutions for this problem (1,2,15-17), it soon becomes apparent that the pertinent independent variable driving the system is the nondimensional product of $\alpha\Delta T$. In contrast, the temperature gradient, g , is a dimensional parameter and is inadequate to describe the system, unless the slab thickness, h , and the system of units used are also specified. For example, if a linear temperature distribution is assumed, g is constant through the thickness,

and

$$\alpha\Delta T = \alpha gh \quad (4)$$

Note that the form of the independent variable, $\alpha\Delta T$, already indicates that an accurate determination of α is just as significant as establishing the value of ΔT . In other words, the sensitivity of the system response to changes in α is just as pronounced as the corresponding sensitivity to variations in ΔT . Therefore, focusing attention and resources on determining ΔT may not be justifiable, unless an equal effort is expended in determining α . Nonetheless, in an analytical study as that presented herein, a constant value of α may be used. Results obtained may easily be adjusted for a different value of α , as necessary.

The self-weight of the slab, determined by γ , must also be accounted for in curling analysis. This is because of (a) the lack of full contact between the subgrade and the slab and (b) the restraint provided by the dead weight to the stress-free curling of the slab into a spherical surface, as predicted by the physics of the problem. The self-weight, however, is of a similar nature as the externally applied wheel loads. Thus, it may be accounted for by adjusting the form of the nondimensional responses and need not be considered as an independent variable.

Reference to analytical studies (2), as well as FE investigations (18), indicates that the sensitivity of the system to the slab size factor, L/l , is significantly more pronounced under a temperature gradient than under flat-slab conditions. A value of L/l between 5 and 8 is usually adequate to give an infinite slab response under no-temperature gradient (13), whereas under curling conditions this ratio is closer to 15.

FINITE ELEMENT FACTORIAL USED

The value of the preliminary considerations presented above is appreciated when examining the factorial that was used to study the response of the system under curling conditions. It was decided to eliminate slab length effects, so an L/l value of about 16 was adopted. The width, W , of the slab was initially set to 144 in. (or $W/l = 3.61$ to 7.66); but to conclude the study, the sensitivity of the calculated responses to this factor was also examined.

The following levels were considered for the other two independent variables:

$$a/l = 0.05, 0.1, 0.2, 0.3, \text{ and}$$

$$\alpha\Delta T = \pm 5.5 \times 10^{-5}, \pm 1.375 \times 10^{-4}, \pm 2.2 \times 10^{-4}$$

For a constant α value of 5.5×10^{-6} ϵ/F , the latter correspond to a temperature differential of ± 10 , ± 25 , and $\pm 40^\circ\text{F}$.

In a preliminary study (4), it was determined that the edge loading condition is critical under curling conditions, as well as under no-temperature differential. Analyses were therefore conducted only for a single square (size $c \times c$) or rectangular (size $2c \times c$) edge load. Thus, using a mere 24 FE runs, it is possible to bracket the vast majority of all conceivable slab, subgrade, and temperature conditions. The only restriction here is the infinite-slab assumption. The input parameters for the 24 cases studied are listed in Table 1.

Finite element program ILLI-SLAB (19,20) was used in this investigation. An iterative procedure is used to account for the effect of temperature curling and to accommodate regaining of subgrade support under load (4). In this respect, the FE formulation used follows closely that proposed by Huang and Wang (21). In designing the FE mesh, guidelines established in earlier studies were followed (20, 22).

ILLI-SLAB RESULTS

Figure 1 summarizes the data obtained for maximum combined normalized tensile stress at top or bottom of the slab for the three daytime and nighttime temperature differentials investigated. A short discussion of these follows.

Positive ΔT : Slab Curled Down (Daytime Conditions)

The maximum combined tensile-bending stress, $\sigma_{t, \max}$, under an edge load on a slab that is curled down occurs at the bottom fiber of the slab at the location of the load. This will be the controlling stress for fatigue calculations because of its magnitude and location, as well as the higher number of traffic loads applied during the day. A much smaller tensile stress also arises at the top fiber of the slab, along the loaded edge at a distance of less than l from the slab corner.

Negative ΔT : Slab Curled Up (Nighttime Conditions)

The maximum combined tensile-bending stress under such conditions generally occurs at the top fiber of the slab, at some distance from the center of the load. This distance is usually between 2 and $4l$, the larger values correspond to low a/l and low $\alpha\Delta T$ values. Exceptions to this general pattern arise for high a/l and low $\alpha\Delta T$ values, when the maximum tensile occurs at the underside of the slab, at the location of the load. In such cases, however, this tensile stress is relatively small, being of the same order of magnitude as Westergaard's prediction ($\Delta T = 0$), and is generally only slightly greater than the corresponding maximum tensile stress arising at the top of the curled slab.

General Discussion of Results

As expected, the absolute value of the nondimensional bending stress ($\sigma h^2/P$) increases dramatically as $\alpha\Delta T$ increases, especially at low a/l values. In all these analyses, the unit weight of concrete, γ , was set at 0.087 pci (or 150 pcf), and its Poisson ratio, μ , was assumed to be 0.15; the maximum stress is normalized in terms of the external load, P , only. Although these choices are fairly inconsequential for the relatively long slabs considered here, a more general and rigorous examination of the nondimensional response would involve, in addition, both γ and μ . Unfortunately this is not feasible at this time.

In comparison, Westergaard's solution ($\Delta T = 0$) is of almost

TABLE 1 FINITE ELEMENT ANALYSES CONDUCTED

RUN	ΔT °F	h in.	E Mpsi	k pci	l in.	L in.	W/l	P kips	c in.	a in.	a/l	σ_t max. psi
1.1	40	10.59	5	200	39.89	630	3.61	1.25	2.5*	1.995	0.05	620
1.2	40	8.23	4	300	28.21	450	5.10	2.5	5	2.821	0.1	595
1.3	40	9.97	3	400	28.21	450	5.10	10	10	5.642	0.2	599
1.4	40	7.16	2	500	18.81	300	7.66	10	10	5.642	0.3	612
2.1	25	10.59	5	200	39.89	630	3.61	1.25	2.5*	1.995	0.05	400
2.2	25	8.23	4	300	28.21	450	5.10	2.5	5	2.821	0.1	413
2.3	25	9.97	3	400	28.21	450	5.10	10	10	5.642	0.2	458
2.4	25	7.16	2	500	18.81	300	7.66	10	10	5.642	0.3	511
3.1	10	10.59	5	200	39.89	630	3.61	1.25	2.5*	1.995	0.05	186
3.2	10	8.23	4	300	28.21	450	5.10	2.5	5	2.821	0.1	234
3.3	10	9.97	3	400	28.21	450	5.10	10	10	5.642	0.2	323
3.4	10	7.16	2	500	18.81	300	7.66	10	10	5.642	0.3	421
4.1	-10	10.59	5	200	39.89	630	3.61	1.25	2.5*	1.995	0.05	-152
4.2	-10	8.23	4	300	28.21	450	5.10	2.5	5	2.821	0.1	-130
4.3	-10	9.97	3	400	28.21	450	5.10	10	10	5.642	0.2	-126
4.4	-10	7.16	2	500	18.81	300	7.66	10	10	5.642	0.3	-140
5.1	-25	10.59	5	200	39.89	630	3.61	1.25	2.5*	1.995	0.05	-370
5.2	-25	8.23	4	300	28.21	450	5.10	2.5	5	2.821	0.1	-308
5.3	-25	9.97	3	400	28.21	450	5.10	10	10	5.642	0.2	-251
5.4	-25	7.16	2	500	18.81	300	7.66	10	10	5.642	0.3	-207
6.1	-40	10.59	5	200	39.89	630	3.61	1.25	2.5*	1.995	0.05	-587
6.2	-40	8.23	4	300	28.21	450	5.10	2.5	5	2.821	0.1	-485
6.3	-40	9.97	3	400	28.21	450	5.10	10	10	5.642	0.2	-372
6.4	-40	7.16	2	500	18.81	300	7.66	10	10	5.642	0.3	-281

Note: For all runs, $\alpha = 5.5 \times 10^{-6} \text{ } \epsilon/\text{ } ^\circ\text{F}$; $\mu = 0.15$; $p = 100 \text{ psi}$; $W = 144 \text{ in.}$; $\gamma = 0.087 \text{ pci} = 150 \text{ pcf}$; $L/l \approx 16$.

* : Load dimensions are $c \times c$, except starred cases for which load dimensions are $2c \times c$.

σ_t max. is a tensile stress occurring at the bottom of the slab for +ve ΔT and at the top of the slab for -ve ΔT .

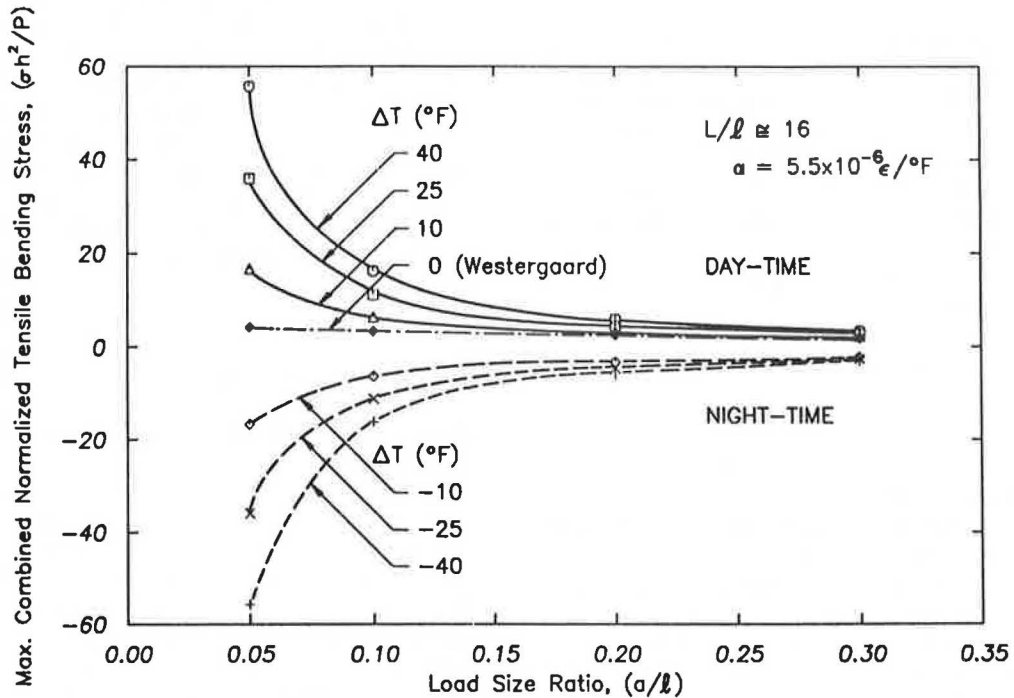


FIGURE 1 Maximum combined normalized tensile stress under edge loading as a function of (a/l) and $(\alpha \Delta T)$.

insignificant magnitude. The ratio, ρ , is defined as

$$\rho = \left(\frac{\sigma_{t, \max}}{\sigma_{t, \text{Wes}}} \right) \quad (5)$$

where $\sigma_{t, \max}$ is the maximum combined tensile stress under curling and load, and $\sigma_{t, \text{Wes}}$ is the maximum tensile stress predicted by Westergaard ($\Delta T = 0$).

It is possible to use FE data to derive a closed-form equation to estimate $(\sigma_{t, \max})$ under any combination of load and temperature conditions. Figure 2 shows the variation of the absolute value of ρ with a/l , for various temperature differentials. It was observed that downward curling (daytime) is slightly more detrimental than upward curling (nighttime). When fatigue consumption is considered, daytime curling will probably be more critical, because of the location of the maximum tension (at the bottom of the slab under the load) and the higher number of applied traffic loads. For these reasons—as a first attempt—the following formula was derived for ρ , based only on the daytime FE results presented in Figure 2:

$$\rho = A + B \{a/l\} + C \{\log_{10}(a/l)\} \quad (6)$$

where A , B , and C are functions of ΔT only, as follows:

$$A = 1.0 - 0.9152 \Delta T \quad (7)$$

$$B = 1.6215 \Delta T \quad (8)$$

$$C = -0.8713 \Delta T \quad (9)$$

Note that Equations 7–9 are presented in terms of ΔT (in $^{\circ}\text{F}$) for clarity, assuming α equals $5.5 \times 10^{-6} \text{ } \epsilon / ^{\circ}\text{F}$. The fundamental relation, of course, involves $\alpha \Delta T$. It would be easy, however, to redefine A , B , and C for any other α value. Furthermore, in certain areas where nighttime truck traffic is significant, its effect on fatigue consumption may also be

accounted for in a fashion similar to that adopted here for the daytime stresses. The form of Equations 6–9 will remain unaltered, and only the nondimensional coefficients will need to be modified for this purpose.

Equation 6 applies to an infinite-slab condition, since an L/l value of about 16 was retained in all the FE runs used in its derivation. A significant decrease in the maximum combined tensile stress may be expected to occur as the slab size decreases below about $L/l = 8$. This is evident if one considers the steep slope of the C -coefficient curve presented by Bradbury (2). In addition, for slabs of infinite length, the maximum combined tensile stress is independent of the chosen value of γ . This, however, is not true for shorter slabs. For the latter, the combined stress is also drastically reduced as γ decreases. This assertion is confirmed by additional FE data, not presented herein.

Thus, the effect of decreasing γ is to make the slab behave as if it were shorter. Stated another way, this implies that the lighter the slab is, the longer it must be before the slab acts as an infinite slab. A theoretical explanation for this is that self-weight in heavy slabs imposes a restraint that is sufficient to ensure full contact under the interior portion of the slab, away from any edges and corners. This support condition was considered by Westergaard (1) as a necessary consequence of the infinite-slab assumption.

The effect of increasing the magnitude of the externally applied load is similar—the higher the applied load, the shorter the L/l value required for infinite-slab conditions. In this sense, the nature of the self-weight of the slab is similar to that of the externally applied load, as stated earlier. Thus, an equation similar to Equation 6 derived for shorter slabs (which would be of greater practical interest) must incorporate the effect of γ . It is expected, however, that this will be achieved by modifying the form of the dependent variable (nondimensional combined bending stress), rather than any of the governing independent variables.

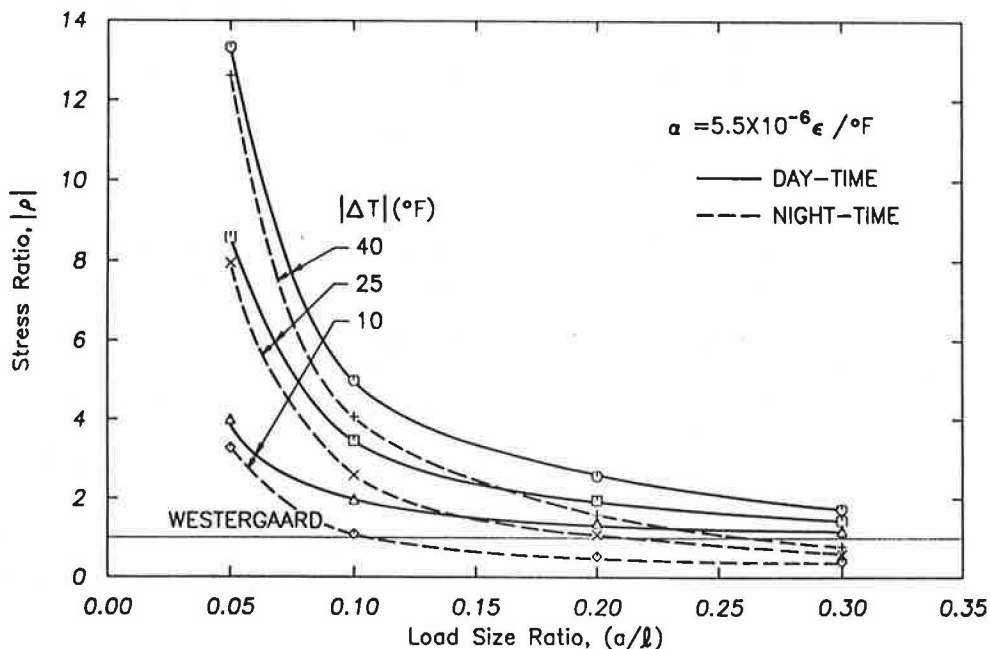


FIGURE 2 Multiplication factor, ρ , for estimating maximum combined tensile stress.

Equation 6 shows that ρ decreases as $\alpha\Delta T$ decreases or as a/l increases. It should be noted that for a/l values larger than about 0.2, Equation 6 suggests that ρ increases as a/l increases, albeit slightly. Any increase, however, is highly questionable and is probably related to the slab size effect mentioned above. Thus, Equation 6 is more reliable for $a/l \leq 0.2$.

Finally, a point needs to be made with respect to the regression technique used to derive Equation 6 from the FE data on which it is based. Twelve observations are considered and the coefficient of determination, R^2 , is 0.985. This is gratifyingly high, but one also must consider the ratio of (predicted/observed) values. These give a mean of 1.005 (cf. 1.00 for a perfect fit) and a coefficient of variation 16 percent (cf. 0.000 for a perfect fit). The latter is, therefore, fairly high. It is only when considering these three statistics together that the goodness of the fit may be evaluated. An R^2 value in the upper nineties is a necessary, but not a sufficient, condition for adequate predictions. This calls for considerable caution (to say the least) when using regression algorithms with significantly lower R^2 values.

Depending on the values of $\alpha\Delta T$ and a/l , stresses as high as 15 times Westergaard's may be obtained. As $\alpha\Delta T$ increases, the turning point in the curves—indicating more pronounced sensitivity to changes in a/l —occurs at increasingly higher values of a/l , as compared to the Westergaard solution. These values are often of considerable practical interest. At a lower $\alpha\Delta T$ and higher a/l , nighttime (upward) curling may result in a lower stress than predicted by Westergaard. The importance of such stress relief in fatigue calculation should not be overestimated, however, because of the location of the maximum stress (at the top fiber at some distance from the load) and the relatively low number of traffic loads applied during the night.

It should be stressed that the form of the independent variable, a/l , implies that the sensitivity of the pavement system response to changes in load radius, a , is just as pronounced as the effect of variations in its radius of relative stiffness, l . Furthermore, altering the value of the load radius causes a more pronounced response change than is effected by varying any one of the individual parameters entering l , (e.g., E , h , and k). This is obvious, since l is the fourth root of the combination of these parameters, while the load radius enters the driving ratio of a/l in its first power.

Compared with Westergaard's solution ($\Delta T = 0$), the sensitivity of the normalized response to changes in a/l , resulting from variations in a or l , is tremendously more pronounced, particularly for a/l values between 0.05 and 0.1. This is the range in which a large number of actual pavements and loads fall.

The preceding considerations suggest that the equivalent single-axle load (ESAL) concept, which states that all traffic loads are reduced to an equivalent single-axle load of a standard weight, is flawed; because it most often implicitly assumes a constant value of load radius. This criticism is not a novel idea. Thirty years ago, in enumerating the limitations of equivalent wheel-load analysis, Yoder (23) listed a number of factors that cause the pavement system to deviate from the assumptions of linear elasticity and full contact, including loss of subgrade strength and plastic subgrade deformation. He also stated that "warping of rigid pavements and subsequent loss of pavement contact must be taken into consideration."

Huang attempted to account for the contact radius in developing equivalency factors (24,25). Although application of the principles of dimensional analysis is evident in Huang's studies, his assumption was that "the change in load factor due to the change in contact radius is not very large so that a straight line interpolation should give a fairly accurate load factor for any other contact radii" (24). This may hold reasonably true for a full-contact analysis, such as Burmister's or Westergaard's, but as the data presented here show, such an expectation is unrealistic when the assumption of full contact is no longer satisfied.

Under linear elastic conditions, a much more fundamental reduction would have been to express mixed, multiple-wheel traffic in terms of an equivalent radius of the applied load. Recent research efforts at the University of Illinois have suggested that it would be possible to derive with reasonable accuracy an equivalent single-axle radius (ESAR) for any arbitrary gear configuration, simply as a function of its geometry (size and spacing of tire prints). This leads to the ESAR concept that offers a unique opportunity for replacing the empirical ESAL approach with a mechanistic procedure.

Even under stress-dependent (nonlinear) conditions, the need to reduce general traffic to an equivalent radius of applied load is still more urgent than the need for an equivalent magnitude of load. The major reason, of course, for the preference given to the ESAL concept is that axle loads are much easier to determine and control than are tire contact radii. Regrettably, the system response is naturally oblivious to matters of practical expediency.

EFFECT OF SLAB WIDTH

In the preceding FE analyses, the slab width, W , was maintained at 144 inches; i.e., the value of W/l (which can be expected to be the more fundamental slab width variable) ranged between 3.61 and 7.66. To examine the effect of slab width, nine additional FE runs were conducted. The results indicated that although the maximum combined normalized bending stress generally increases as W/l increases, this effect becomes negligible for W/l values in excess of about 3.5. The 24 cases considered above are, therefore, judged to be fairly insensitive to this effect.

RECONSIDERATION OF ZERO-MAINTENANCE RESULTS

The dimensional analysis approach to data interpretation presented above may be applied in a re-examination of existing data bases. As an illustration, the data base generated by the zero-maintenance (ZM) study (18) was selected, because it was one of the largest available. The data consisted of analytical results, obtained by performing a series of runs, using an FE program developed at the University of Kentucky by Huang and Wang (21). This is a precursor to ILLI-SLAB and is sometimes referred to as KENWINK. For the case of an 18-kip single-axle load perpendicular to the longitudinal slab edge, the data base included a complete factorial of 432 runs for the following factors and levels:

Slab thickness, $h = 8, 10, \text{ and } 14 \text{ in.}$,
 Subgrade modulus, $k = 50, 200, \text{ and } 500 \text{ pci}$,
 Thermal gradient, $g = -1.5, 0, \text{ and } +3.0^\circ\text{F/in.}$,
 Slab length, $L = 15, 20, 25, \text{ and } 30 \text{ ft}$, and
 Erodability, $e_s: 0, 12, 36, \text{ and } 60 \text{ in.}$

The slab considered consisted of one layer with a modulus, E , of $5.0 \times 10^6 \text{ psi}$ and a Poisson ratio, μ , of 0.15. The concrete coefficient of thermal expansion, α , was set at $5.0 \times 10^{-6} \text{ } \epsilon/^\circ\text{F}$. The unit weight of concrete used was not explicitly stated but this was probably 150 pcf. The width of the slab, W , was held constant at 144 in. ($W/l = 2.071 \text{ to } 5.602$). The load was applied by two wheels, each 15 by 12 in. at a center-to-center spacing, S , of 78 in. ($S/a = 10.3$) under 50 psi of pressure. The FE mesh used was relatively coarse, and some detrimental effects of this factor on the results obtained are discussed below.

Note that the ZM factorial is considerably longer than the ILLI-SLAB factorial presented earlier, but this is primarily a consequence of the implicit assumption that h , k , and g are fundamental independent variables. It is clear now that this is not the case, because the independent variables have been shown to be the nondimensional ratios, a/l and $\alpha\Delta T$, while h , k , and g are merely input parameters. Furthermore, the effect of the slab size is purportedly accounted for by the input parameter, L , whereas the fundamental independent variable is the nondimensional ratio L/l . Similarly, the effect of the loss of subgrade support in a longitudinal strip along the loaded slab edge was investigated during the ZM study in terms of the erodability, e_s . This gives the width of a zero-subgrade modulus strip along the loaded edge (in inches). It

may be postulated that the independent variable governing this aspect of the response is the nondimensional ratio, e_s/l .

For the case of no-temperature differential, Figure 3 compares the Westergaard solution and the ZM FE results for different values of the erodability ratio, e_s/l . On the basis of an earlier investigation (14), and for the sake of simplicity, the effect of the second tire may be considered negligible in calculating the Westergaard response. Thus, the solution shown in Figure 3 assumes a total load, P , of 9,000 pounds, applied over a circle, radius $a = 7.57 \text{ in.}$, under a uniform pressure, p , of 50 psi. Also note that the original data in the ZM report were extrapolated to yield the values corresponding to the rounded e_s/l values shown in Figure 3.

As expected, as e_s/l increases, the nondimensional maximum combined tensile stress arising in the slab increases substantially. The ZM report gave no indication as to the location of this stress (i.e., whether it occurs at the edge under the load or elsewhere) at the top or bottom fiber of the slab. Such information is essential in calculating fatigue consumption.

Comparing the curve for $e_s/l = 0$ to the Westergaard curve in Figure 3, provides an estimate of the effects of the FE mesh used. Good agreement is obtained at high values of a/l , due to the corresponding high L/l values (Westergaard assumes an infinite slab). For intermediate a/l values, the FE results are about 10 percent higher than Westergaard's. This discrepancy is due to the coarseness of the mesh in the vicinity of the load (26).

Finally, the curve for $e_s/l = 0$ bends over toward the Westergaard curve at low a/l , but this is not an indication of better agreement between the two solutions. Rather, it is due to the low L/l values, corresponding to these a/l values. The ZM results suggest that, for $\Delta T = 0$, results are not affected by

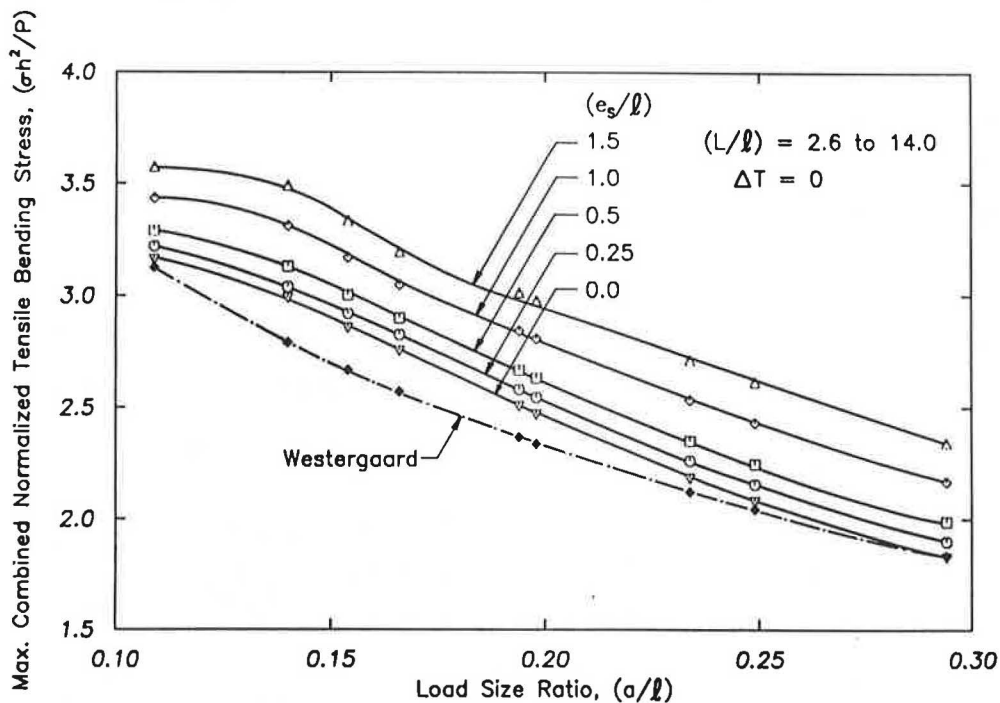


FIGURE 3 Zero maintenance results for $\Delta T = 0$: effect of erodability.

changes in slab size. This, of course, is only true for L/l in excess of about 5, and is certainly inapplicable in the case of L/l values as low as 2.588, associated with some low a/l results in Figure 3.

Notwithstanding these limitations, Figure 3 provides a concise graphic depiction of the effect of erodability on the maximum bending stress. When the data are presented in this fashion, responses may be predicted for cases involving values of the individual parameters (e.g., a , P , E , μ , h , k , and e_s) other than those on which Figure 3 is based. Four separate figures are used in the ZM report (18) to present the data obtained; each is applicable to a specific combination of the input parameters.

Using the dimensional analysis approach, the same data are replotted in a single graph (Figure 3). In this graph, the data line up to form smooth continuous curves, even though points on the same curve assume different input parameters, such as k and h . This confirms the validity of the proposed interpretation method. Figure 3 also allows a direct comparison with Westergaard, and an estimation of the error introduced by the characteristics of the FE mesh.

For the case of full subgrade support ($e_s/l = 0$), Figures 4 through 6 show the effect of slab size on the nondimensional combined maximum tensile stress under edge loading and a temperature differential. This stress is plotted versus a/l , for various values of L/l and $\alpha\Delta T$. Once again, the raw ZM data were extrapolated to give the responses at the rounded L/l values shown in these figures.

In examining these results, it was observed that for the dead and wheel loads considered there is a limiting value of L/l beyond which the slab behaves as an infinite slab. This value is also a function of a/l and $\alpha\Delta T$, but the effect of a/l is quite negligible. It is noted that the limiting L/l value is slightly more sensitive to changes in $\alpha\Delta T$ when considering upward curling (nighttime). Under both night and day temperature

differentials, a slab size of $15l$ or more may be necessary for infinite-slab response. This validates the choice made earlier in performing the runs for the ILLI-SLAB factorial.

The ZM results suggest that limiting the L/l ratio to about 4 will ensure that the combined stresses under $\Delta T = +30^\circ\text{F}$ (or less) will not exceed a value equal to about twice that predicted by Westergaard. This seems to hold reasonably true for any load size ratio a/l . Allowing the L/l ratio to reach 8 will cause a stress that is three times as large as Westergaard's. Thus, it appears necessary to reconsider conventional practice with respect to the selection of maximum slab size. The prevalent recommendation in the United States is that L (in feet) should not exceed 1.75 times the thickness, h , of the slab (in inches), or $L/h \leq 21$. On the other hand, recent European experience (27,28) suggests a somewhat longer maximum slab length, or $L/h \leq 25$.

The fact that the pertinent fundamental engineering independent variables are not L and W , but the nondimensional ratios, L/l and W/l , clearly means that any criteria developed cannot be expressed in terms of dimensional quantities (e.g., W equals 14 ft). The slab dimensions in feet cannot be determined until the properties of pavement, including its support, are known. Furthermore, it is evident that a criterion in terms of L/h , say, is much more relevant, because it accounts for the most important property of the slab, namely its thickness. Nonetheless, it is interesting to observe that such properties as E and k are not reflected in such a criterion either. It is therefore not surprising that the U.S. and European experience differs somewhat. This is presumably in response to the different soil conditions and concrete mixing practices in these two parts of the world.

Figure 7 compares the L/h criteria most commonly used in the United States and in Europe to the proposed L/l criterion (29). Contrary to the implication of an L/h design criterion, size-related problems may arise in a pavement as k increases.

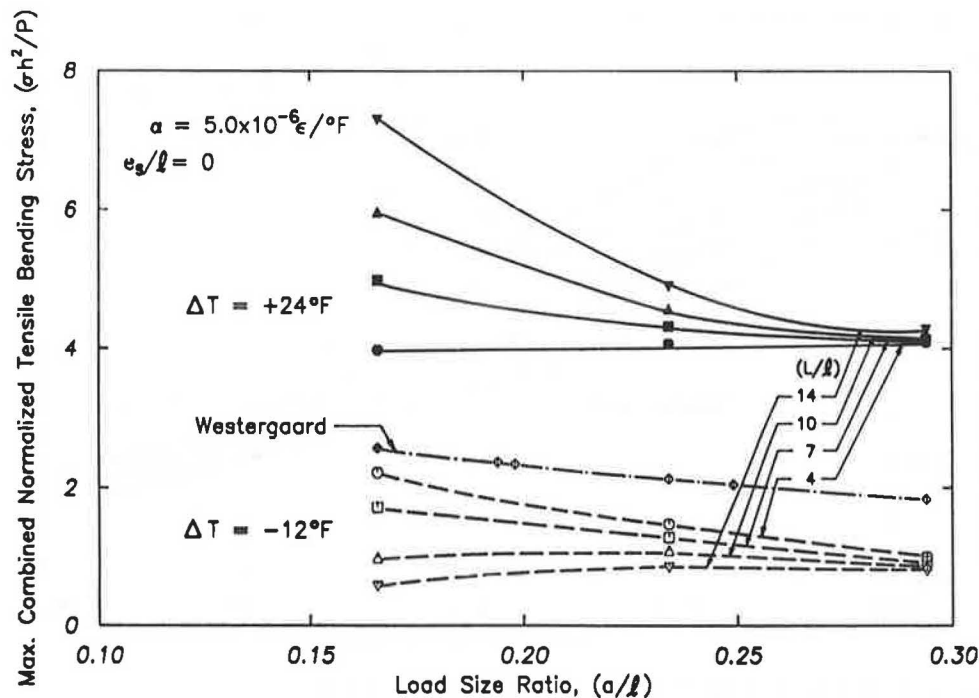


FIGURE 4 Effect of slab size: $\Delta T = -12$ and $+24^\circ\text{F}$.

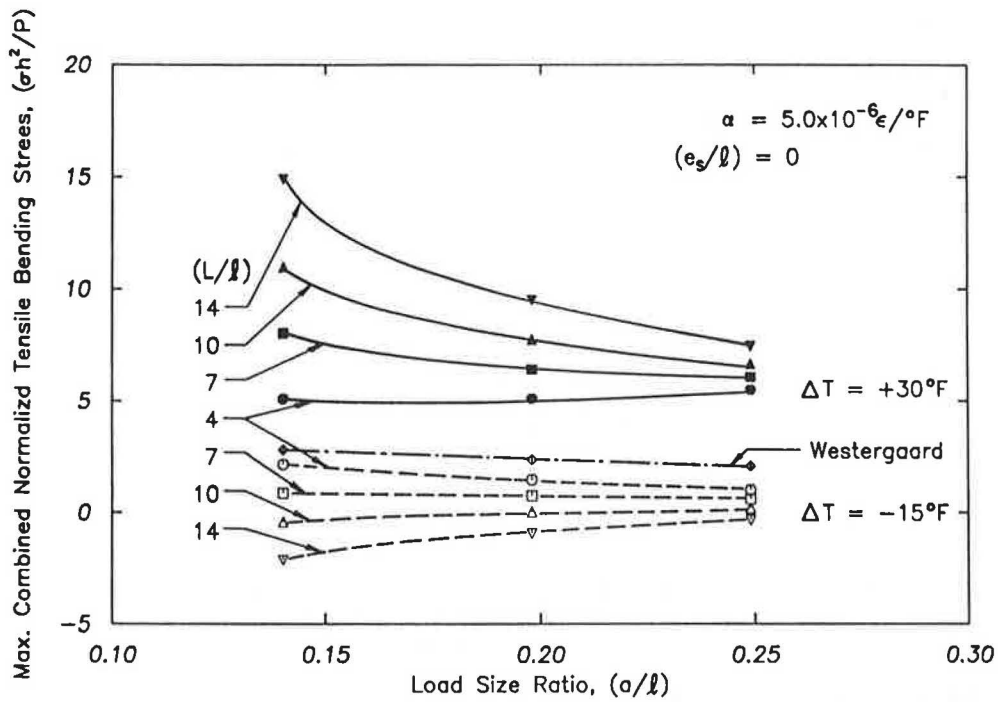


FIGURE 5 Effect of slab size: $\Delta T = -15$ and $+30^\circ F$.

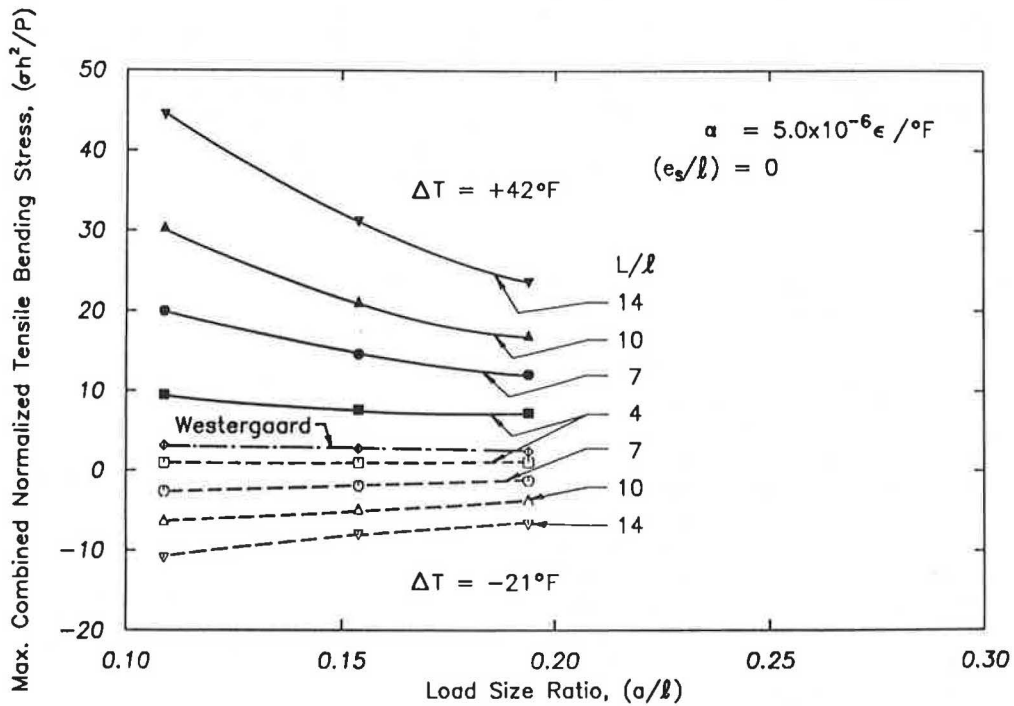


FIGURE 6 Effect of slab size: $\Delta T = -21$ and $+42^\circ F$.

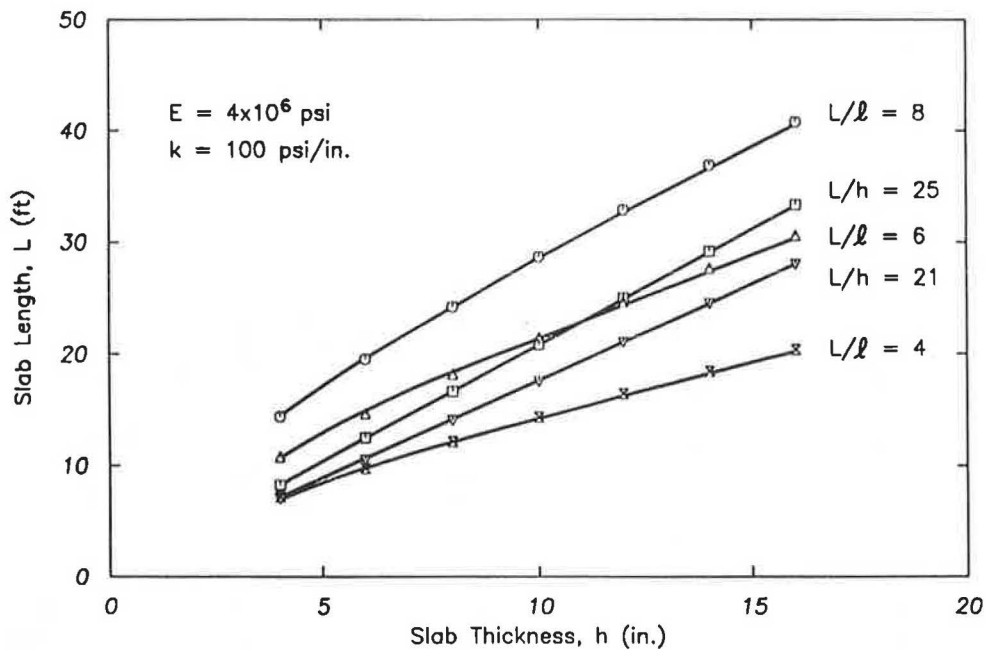


FIGURE 7 Comparison of slab length criteria (29).

It is also evident that decreasing E will have a similar effect. In contrast, an L/l criterion will result in shorter slabs under both of these conditions. Another interesting observation is that slab lengths determined according to the two L/h criteria lie for the most part within the range defined by $L/l = 4$ and $L/l = 6$. Thus, the former is shown to be a fairly conservative choice, while $L/l = 5$ appears to be a promising alternative. The ultimate choice, of course, should be tested against local experience. As noted earlier, the maximum combined tensile stress increases at a decreasing rate as W increases, tending to a constant value at about $W/l = 4$. This gives support to setting $L = W$.

CONCLUSION

The purpose of this paper has been twofold: (a) to present a solution to the problem of a slab-on-grade under combined temperature and wheel loading, and, just as importantly, (b) to propose a sound engineering approach to numerical, experimental, and field data interpretation. The principles of dimensional analysis, so fruitfully used in other branches of engineering, have largely been ignored in transportation facilities studies, particularly since the introduction of computers in the early 1960s. Despite occasional and admirable exceptions, the general trend in the last three decades has been to show an overwhelming preference for and an unlimited confidence in the results of sophisticated statistical analyses—without much consideration of the underlying engineering interactions among the host of input parameters involved.

Although in a highly empirical field, such as the study of pavement behavior, regression techniques will always be an invaluable tool, the profession can benefit immensely by using dimensional analysis to determine the engineering dependent and independent variables to be examined. Without such

exercise of engineering judgment, regression is lamentably bound to remain just that.

ACKNOWLEDGMENTS

The investigations for this paper were conducted under a research project sponsored by FHWA, U.S. Department of Transportation. Carol A. Nolan was the project administrator, and Stephen W. Forster was the contracting officer's technical representative. The useful comments of M. I. Darter and Roger M. Larson, and the assistance of Lynn Kastel in drafting the figures, are greatly appreciated.

REFERENCES

1. H. M. Westergaard. Analysis of the Stresses in Concrete Roads Caused by Variations in Temperature. *Public Roads*, Vol. 8, No. 3, May 1927, pp. 54–60.
2. R. D. Bradbury. *Reinforced Concrete Pavements*. Wire Reinforcement Institute, Washington, D.C., 1938.
3. L. W. Teller and E. C. Sutherland. The Structural Design of Concrete Pavements. *Public Roads*, Vol. 16, No. 8, Oct. 1935, pp. 145–158; Vol. 16, No. 9, Nov. 1935, pp. 169–197; Vol. 16, No. 10, Dec. 1935, pp. 201–221; Vol. 17, No. 7, Sept. 1936, pp. 175–192; Vol. 23, No. 8, April, May, June 1943, pp. 167–212.
4. G. T. Korovesis and A. M. Ioannides. Discussion of "Effect of Concrete Overlay Debonding on Pavement Performance," by T. Van Dam, E. Blackmon, and M. Y. Shahin. In *Transportation Research Record 1136*, TRB, National Research Council, Washington, D.C., 1987, pp. 129–132.
5. J. A. Roberson and C. T. Crowe. *Engineering Fluid Mechanics*, 2nd ed., Houghton Mifflin Company, Boston, Mass., 1980.
6. D. M. Burmister. The Theory of Stresses and Displacements in Layered Systems and Applications to the Design of Airport Runways. *HRB Proc.*, Vol. 23, 1943, pp. 126–148.

7. D. M. Burmister. Open Floor Discussion, Session 1, *Proc., 1st International Conference on the Structural Design of Asphalt Pavements*. University of Michigan, Ann Arbor, 1962, p. 15.
8. J. B. Rauhut, J. C. O'Quin, and W. R. Hudson. Sensitivity Analysis of FHWA Structural Model VESYS IIM. In *Proc., 4th International Conference on the Structural Design of Asphalt Pavements*, University of Michigan, Ann Arbor, Vol. I, 1977, pp. 139–147.
9. A. M. Ioannides. Dimensional Analysis in NDT Rigid Pavement Evaluation. *Journal of Transportation Engineering*, ASCE (In press).
10. A. M. Ioannides. Discussion of "Response and Performance of Alternate Launch and Recovery Surfaces that Contain Layers of Stabilized Material," by R.R. Costigan and M.R. Thompson, In *Transportation Research Record 1095*, TRB, National Research Council, Washington, D.C., 1986, pp. 70–71.
11. A. M. Ioannides. *Analysis of Slabs-on-Grade for a Variety of Loading and Support Conditions*. Ph.D. thesis. University of Illinois, Urbana, Ill., 1984.
12. A. M. Ioannides. Finite Difference Solution for Plate on Elastic Solid. *Journal of Transportation Engineering*, ASCE, Vol. 114, No. 1, Jan. 1988, pp. 57–75.
13. A. M. Ioannides, M. R. Thompson, and E. J. Barenberg. Westergaard Solutions Reconsidered. In *Transportation Research Record 1043*, TRB, National Research Council, Washington, D.C., 1985, pp. 13–23.
14. A. M. Ioannides. Discussion of "Thickness Design of Roller-Compacted Concrete Pavements," by S.D. Tayabji and D. Halpenny. In *Transportation Research Record 1136*, TRB, National Research Council, Washington, D.C., 1987, pp. 31–32.
15. J. Thomlinson. Temperature Variations and Consequent Stresses Produced by Daily and Seasonal Temperature Cycles in Concrete Slabs. *Concrete and Constructional Engineering*, Vol. 35, No. 6, June 1940, pp. 298–307 and Vol. 35, No. 7, July 1940, pp. 352–360.
16. S. G. Bergström. Temperature Stresses in Concrete Pavements. *Proceedings No. 14 (Handlingar)*, Swedish Cement and Concrete Research Institute at the Royal Institute of Technology, Stockholm, Sweden, 1950.
17. K. H. Lewis and M. E. Harr. Analysis of Concrete Slabs on Ground Subjected to Warping and Moving Loads. In *Highway Research Record 291*, HRB, National Research Council, Washington, D.C., 1969, pp. 194–211.
18. M. I. Darter. *Design of Zero-Maintenance Plain Jointed Concrete Pavement: Vol. I—Development of Design Procedures*. Report FHWA-RD-77-111. Federal Highway Administration, Washington, D.C., June 1977.
19. A. M. Tabatabaie and E. J. Barenberg. Structural Analysis of Concrete Pavement Systems. *Transportation Engineering Journal*, ASCE, Vol. 106, No. TE5, Sept. 1980, pp. 493–506.
20. A. M. Ioannides, M. R. Thompson, and E. J. Barenberg. Finite Element Analysis of Slabs-On-Grade Using a Variety of Support Models. In *Proc., Third International Conference on Concrete Pavement Design and Rehabilitation*, Purdue University, April 23–25, 1985, pp. 309–324.
21. Y. H. Huang and S. T. Wang. Finite-Element Analysis of Rigid Pavements with Partial Subgrade Contact. In *Transportation Research Record 485*, TRB, National Research Council, Washington, D.C., 1974, pp. 39–54.
22. A. M. Ioannides. The Problem of a Slab on an Elastic Solid Foundation in the Light of the Finite Element Method. In *Proc., 6th International Conference on Numerical Methods in Geomechanics*, Paper No. 408, Innsbruck, Austria, April 11–15, 1988, pp. 1059–1064.
23. E. J. Yoder. *Principles of Pavement Design*. John Wiley and Sons, Inc., New York, 1959.
24. Y. H. Huang. Chart for Determining Equivalent Single-Wheel Loads. *Journal of the Highway Division*, ASCE, Vol. 94, No. HW2, November 1968, pp. 115–127.
25. Y. H. Huang. Computation of Equivalent Single-Wheel Loads Using Layered Theory. In *Highway Research Record 291*, HRB, National Research Council, Washington, D.C., 1969, pp. 144–155.
26. A. M. Ioannides. Insights from the Use of Supercomputers in Analyzing Rigid and Flexible Pavements. Presentation to Committee on Rigid Pavements (A2B02), 66th Annual Meeting of the Transportation Research Board, Washington, D.C., January 1987.
27. J. Eisenmann. Discussion, Session 1B: Westergaard Theories. Workshop on Theoretical Design of Concrete Pavements. Epen, The Netherlands, June 5–6, 1986.
28. A. Lampinen. Design of Concrete Pavements in Finland. Workshop on Theoretical Design of Concrete Pavements. Epen, The Netherlands, June 5–6, 1986.
29. A. M. Ioannides and R. A. Salsilli-Murua. *Slab Length, Slab Width and Widened Lanes Effects in Rigid Pavements*. University of Illinois, Urbana, Ill., 1988.

Publication of this paper sponsored by Committee on Rigid Pavement Design.